Hydraulics of skimming flows over stepped channels and spillways

Hydraulique des écoulements extrémement turbulents sur des canaux en marches d'escalier

HUBERT CHANSON
Lecturer in Hydraulics/Fluid mechanics,
Department of Civil Engineering,
The University of Queensland,
Brisbane QLD 4072, Australia

SUMMARY
Stepped chutes have become recently a popular method for discharging flood waters. The steps increase significantly the rate of energy dissipation taking place on the spillway face and reduce the size of the required downstream energy dissipation basin. This paper reviews the hydraulic characteristics of skimming flows. The onset of skimming flows is discussed. New results are presented to estimate the flow resistance along stepped chutes. The study indicates some major difference between the flow patterns on steep and flat stepped chutes. An analogy with flow over large roughness is developed. Then the calculations of the start of air entrainment are detailed. The results indicate that free surface aeration occurs much more upstream than on smooth spillways. The effects of flow aeration are later discussed.

RÉSUMÉ
Récemment, il est devenu courant de concevoir des évacuateurs de crues en marches d'escalier. Les marches d'escalier augmentent considérablement la dissipation d'énergie au long du coursier, et permettent de réduire la taille des bassins de dissipation avals. Le présent article décrit les caractéristiques hydrauliques des écoulements extrémement turbulents sur des coursiers en marches d'escalier. On discute les conditions d'apparition des écoulements extrémement turbulents. Puis on présente de nouveaux résultats, permettant d'estimer les coefficient de pertes de charge. Cette étude montre une différence de comportement des écoulements entre des pentes faibles et fortes. Une analogie avec des écoulements sur de grandes rugosités est aussi présentée. Puis on décrit les caractéristiques du point d'appariton de l'eau blanche. Enfin, les effets de l'entraînement d'air dans l'écoulement sont brièvement discutés.

1 Introduction

1.1 *Applications of stepped chutes*

For the last decades, stepped spillways have become a popular method for handling flood releases (Fig. 1). The steps increase significantly the rate of energy dissipation taking place along the spillway face and reduce the size and the cost of the downstream stilling basin. The development of new construction materials (e.g. roller compacted concrete RCC, gabion) has increased the interest for stepped spillways. The construction of stepped spillway is compatible with the slip-forming and RCC placing methods (e.g. Monksville dam, USA, M'Bali dam, RCA). Also gabion stepped spillways are the most common type of spillways used for gabion dams (e.g. Rietspruit outfall, SA).

Stepped channels can also be used to increase the discharge capacity. In USSR, Soviet engineers

Revision received October 25, 1993. Open for discussion till December 31, 1994.

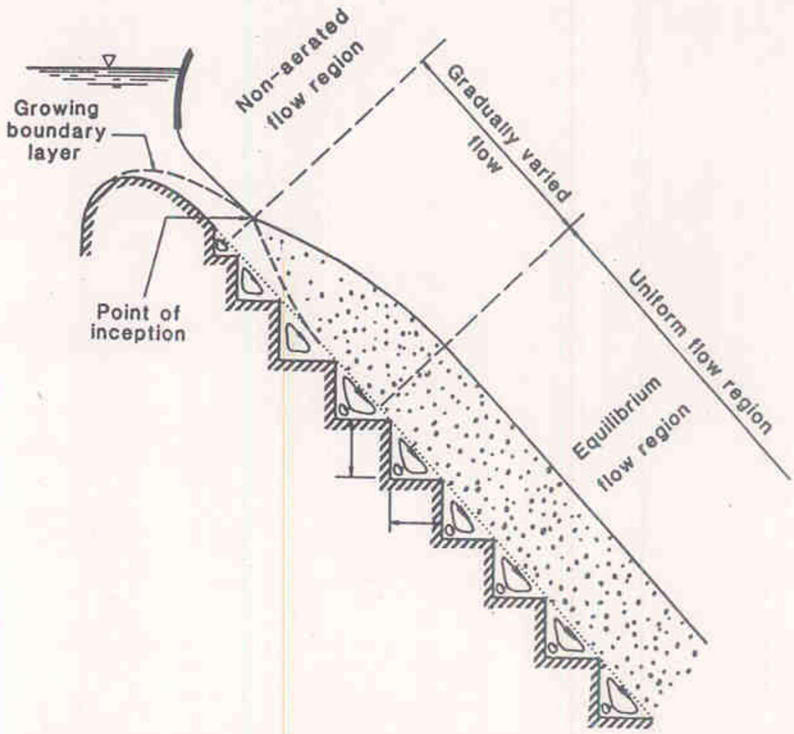

Fig. 1. Skimming flow above a stepped spillway.

developed the concept of overflow earth dam (Grinchuk et al. 1977, Pravdivets and Bramley 1989). The spillway consists of a revetment of precast concrete blocks laid on a filter and erosion protection layer. The channel bed is very flexible and allows differential settlements : individual blocks do not need to be connected to adjacent blocks. More high discharge capacity is achieved (i.e. up to 60 m^2/s). The high degree of safety allows the use of such channels as primary spillways (Pravdivets and Bramley 1989).

Stepped cascades are utilised also in water treatment plants. As an example, five artificial cascades were designed along a waterway system to help the re-oxygenation of the polluted canal (Gasparotto 1992). The waterfalls were landscaped as leisure parks and combined flow aeration and aesthetics. Aesthetical applications of stepped cascades can include stepped fountains in cities (e.g. in Brisbane, Hong Kong, Taipei).

In this paper, the author reviews the hydraulic characteristics of skimming flows over stepped chutes. A re-analysis of model and prototype data (Table 1) is presented. The results provide information on the onset of skimming flow and on the flow resistance in stepped channels. Then the flow conditions at the point of inception of air entrainment are described. Considerations on energy dissipation and the effects of air entrainment are discussed briefly.

It must be noted that this paper presents results obtained for chutes with horizontal steps. Essery and Horner (1978), Peyras et al. (1992) and Frizell (1992) discussed experimental results obtained with inclined and pooled steps.

1.2 *History of stepped spillways*

The world's oldest stepped spillways are probably the spillways of the Khosr River dams, Iraq. The Khosr River dams were built around B.C. 694 by the Assyrian King Sennacherib. The dams were designed to supply water to the Assyrian capital city Nineveh (near the actual Mosul).

Remains of the dams are still in existence (Smith 1971). Both dams feature a stepped downstream face and were intended to discharge the river over their crests.
Much later, the Romans built stepped overflow dams in Syria and Tunisia (Table 2). After the fall of the Roman empire, Moslem civil engineers gained experience from the Nabateans, the Romans and Sabeans. Stepped spillways built by the Moslems can be found in Iraq and in Spain. After the Reconquest of Spain, Spanish engineers benefited from the Roman and Moslem precedents. In 1791, they built the largest dam with a stepped spillway, but the dam was washed out in 1802 after a foundation failure.

Table 1. Characteristics of model and prototype studies
Caractéristiques d'études sur modèle et prototype

reference	slope (deg.)	scale	step height h (m)	Nb of steps	discharge q_w (m^2/s)	flow regime	remarks
Model studies							
Essery and Horner (1978)	11 to 40		0.03 to 0.05	4 to 18		nappe and skimming	CIRIA tests (UK). Include inclined steps.
Noori (1984)	5.7		0.004	100	0.007 to 0.09	skimming	(UK). $W = 0.5$ m.
	11.3		0.013	70	0.025 to 0.2		
Sorensen (1985)	52.05	1/10	0.061	11	0.006 to 0.28		Monksville dam spillway model (USA). $W = 0.305$ m.
		1/25	0.024	59	0.006 to 0.28	nappe and skimming	
Diez-Cascon et al. (1991)	53.1	1/10	0.03–0.06	50 to 100	0.022 to 0.28	skimming	(Spain). $W = 0.8$ m.
Bayat (1991)	51.3	1/25	0.024		0.006 to 0.07		Godar-e-landar spillway model (Iran). $W = 0.3$ m.
			0.03				
			0.02				
Frizell and Mefford (1991)	26.6		0.051	47	0.077	skimming flow	USBR research laboratory (USA). $W = 0.457$ m.
Peyras et al. (1991, 1992)	18.4, 26.6, 45	1/5	0.20	3, 4, 5	0.04 to 0.27	nappe and skimming	Gabion stepped chute (France). $W = 0.8$ m.
Beitz and Lawless (1992)	51.3 and 48.0	1/60	0.02	10	6E-4 to 0.093	nappe and skimming	2-D model of the Burton Gorge dam (Australia).
Frizell (1992)	26.6		0.051	47	0.577		USBR research laboratory (USA). $W = 0.457$ m.
Bindo et al. (1993)	51.34	1/21.3	0.038	31–43	0.01 to 0.142	skimming	M'Bali spillway model (France). $W = 0.9$ m.
		1/42.7	0.019	43	0.007 to 0.04	skimming	
Christodoulou (1993)	55.0		0.025	15	0.02 to 0.09	skimming	$W = 0.5$ m.
Prototype studies							
Grinchuk et al. (1977)	8.7	N/A	0.41	12	1.8 to 60	skimming	Dneipr hydro plant (USSR). Full-scale test. $W = 14.2$ m.

In all early dams (Table 2), stepped spillways were selected to contribute to the stability of the dam, for their simplicity of shape or for a combination of the two. The spillway of the New Croton dam (1906) is probably the first stepped chute designed specifically to dissipate flow energy.

Table 2. Historical stepped spillways
Evacuateurs de crues en marches d'escalier dans l'histoire

name	year	ref.	dam height (m)	slope (deg.)	construction	comments, discharge
River Khosr dams	B.C. 694	[1, 2]	2.9		Masonry of limestone, sandstone mortared together.	Built by the Assyrian King Sennacherib to supply water to his capital city Nineveh. Discharge over the dam crest. Lower dam.
			>1.4	30		Upper dam. 5 steps.
Kasserine dam	A.D. 100?	[1]	10	57	Cut and fitted masonry blocks with mortared joints used to face a rubble and earth core.	Roman dam 220 km SW of Tunis, Tunesia. 6 steps followed by an overfall. Discharge over the dam crest. $W=150$ m.
Qasr Khubbaz	A.D. 100/200	[3]	6.1		Masonry dam with limestone slabs.	Roman dam in Syria, on the Euphrate rivver. Reservoir capacity: 9000 m^3 of water.
Mestella dam	A.D. 960	[1]	2.1	27	Rubble masonry and mortar core faced with large masonry blocks and mortared joints.	Built by the Moslims in Spain. Stepped weir: $W=73$ m. Maximum discharge: around 4000 m^3/s (?).
Adheim dam	1300?	[1]	15.2	51	Masonry steps.	Built by the Moslims during the Sassanian period in Iraq.
Almansa dam	1384?	[1]	15	40	Rubble masonry with a facing of large masonry blocks.	In Spain. Discharge over the dam crest. Broad crest followed by 14 steps and an overfall.
Puentes dam	1791	[1]	50	51	Rubble masonry core set in mortar and faced with large cut stones. Dam failure in 1802.	Dam across the Rio Guadalentin, Spain. Discharge over the crest. 4 steps followed by 59 degree uniform slope. Step height: $h=4.175$ m.
New Croton dam	1906	[4]	53		Masonry. Dam failure in 1955.	USA. Maximum discharge: 1650 m^3/s. $W=305$ m.

Note: [1] Smith (1971); [2] Forbes (1955); [3] Stein (1940); [4] Wegmann (1907).

1.3 *Flow regimes*

The flow over stepped chutes can be divided into nappe flow regime and skimming flow regime (Fig. 2). In the nappe flow regime, the water proceeds in a series of plunges from one step to another. At the brink of each step, the flow becomes a free-falling jet before impinging the next

step. Energy dissipation occurs by jet breakup and jet mixing on the step, and with the formation of a partial or fully developed hydraulic jump on the step (Fig. 2a). Essery and Horner (1978), Peyras et al. (1991) and Chanson (1993) have detailed the flow properties of nappe flow regime. In a skimming flow regime, the water flows down the stepped face as a coherent stream skimming over the steps and cushioned by the recirculating fluid trapped between them (Fig. 2b). The external edges of the steps form a pseudo-bottom over which the flow pass. Beneath this, horizontal axis vortices develop and are maintained through the transmission of shear stress from the fluid flowing past the edge of the steps.
For a stepped spillway with skimming flow regime, the free-surface of the flow is smooth in the early steps and no air entrainment occurs. Next to the boundary however, turbulence is generated. When the outer edge of the turbulent boundary layer reaches the free surface, air entrainment at the free surface occurs (Fig. 1). Downstream of the point of inception of air entrainment, the flow becomes rapidly aerated as shown by photographs (Krest'yaninov and Pravdivets 1986, Diez-Cascon et al. 1991, Peyras et al. 1991).

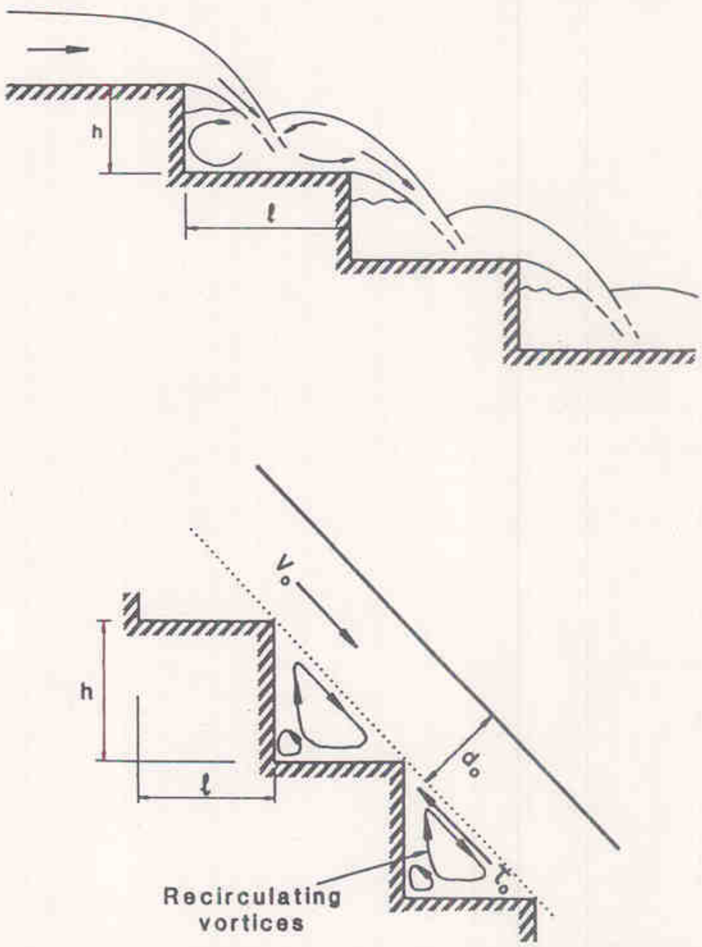

Fig. 2. Flow regimes above stepped channel: (a) nappe flow; (b) skimming flow.

2 Onset of skimming flows

For small discharges and flat slopes, the water flows as a succession of waterfalls (i.e. nappe flow regime). An increase of discharge or of slope might induces the apparition of skimming flow regime. The onset of skimming flow is a function of the discharge, the step height and length. The author re-analysed experimental data obtained by Essery and Horner (1978), Degoutte et al. (1992) and Beitz and Lawless (1992) (Fig. 3). For these data, skimming flow regime occurs for discharges larger than a critical value defined as:

$$\frac{(d_c)_{onset}}{h} = 1.057 - 0.465 * \frac{h}{l} \tag{1}$$

where h is the step height, l is the step length and $(d_c)_{onset}$ is the characteristic critical depth. It must be noted that equation [1] was deduced for h/l ranging from 0.2 to 1.3. It should not be used outside that range without great care.

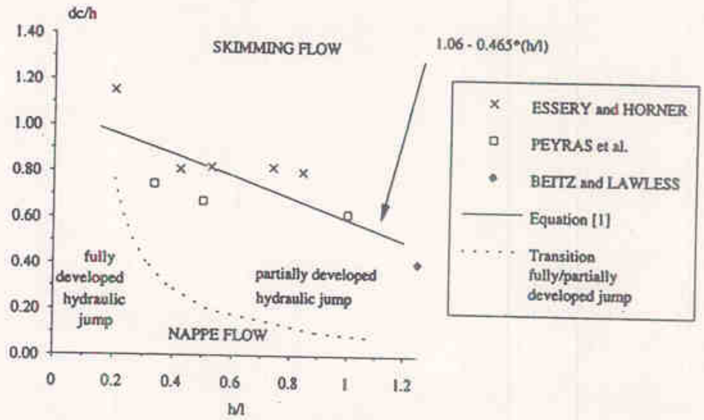

Fig. 3. Onset of skimming flow regime.

In flat channels with strip bottom roughness, Adachi (1964) and Knight and MacDonald (1979) observed also stable circulatory motion in the grooves between adjacent elements for subcritical flows. But during these experiments, the occurrence of "quasi-smooth flow" was independent of the flow rate and was a function only of the ratio of the roughness spacing over roughness height (i.e. Spacing/Height ≤ 3.4). O'Loughlin and MacDonald (1964) studied flows past cubical roughness elements and observed a stable recirculatory flow pattern for roughness densities larger than 0.25. In pipe flows, Levin (1968) analysed head losses caused by grooves perpendicular to the flow. He found that the effect of the grooves on the head loss is small if the length of the cavity over its depth is less than 4. It is interesting to note the close agreement between the observations of Adachi (1964), O'Loughlin and MacDonald (1964), Levin (1968) and Knight and MacDonald (1979).

In horizontal channels and pipes, the onset of "quasi-smooth flow" over artificial roughness corresponds to the apparition of stable recirculation vortices. On stepped channels, it will be shown (paragraph 3) that skimming flows may occur with stable and unstable recirculation eddies in the cavities. Hence it is not possible to compare the apparition of stable recirculation vortices with the onset of skimming flow and the disappearance of nappe flows.

3 Flow resistance of skimming flows

3.1 *Introduction*

For a skimming flow regime, horizontal vortices develop beneath the pseudo-bottom formed by the external edges of the steps. The vortices are maintained through the transmission of turbulent shear stress between the skimming stream and the recirculating fluid underneath (Fig. 2b). Several author studied "quasi-smooth flows" past strip roughness in pipes and open channels. Their results indicated that the classical flow resistance calculations must be modified to take into account the shape of the large roughness elements. The flow resistance is the sum of the skin resistance and the form resistance of the steps. The geometry of a step is characterised by its depth normal to the streamlines (i.e. $k_s = h * \cos\alpha$) and the channel slope (i.e. $\tan\alpha = h/l$). Neglecting the effects of flow aeration, dimensional analysis yields:

$$f = f_1\left(\frac{k_s'}{D_H};\ Re;\ \frac{k_s}{D_H};\ \frac{h}{l}\right) \tag{2}$$

where f is the friction factor, k_s' is the surface (skin) roughness, Re is the Reynolds number and D_H is the hydraulic diameter.

3.2 *Experimental data*

If uniform flow conditions are reached along a constant slope channel, the friction factor can be deduced from the momentum equation as (Chanson 1993):

$$f = \frac{8 * g * \sin\alpha * d_0^2}{q_w^2} * \frac{D_H}{4} \tag{3}$$

where g is the gravity constant, d_0 is the uniform flow depth and q_w is the discharge per unit width. For non-uniform gradually varied flows, the friction factor can be deduced from the energy equation:

$$f = \frac{8 * g * d^2}{q_w^2} * \frac{D_H}{4} * \frac{\Delta H}{\Delta s} \tag{4}$$

where ΔH is the total head loss over a distance Δs. $(\Delta H/\Delta s)$ is the friction slope (Henderson 1966). The author re-analysed model and prototype data using equations [3] and [4]. Details of the flow conditions are reported in Table 1. The analysis indicates that the friction factor for these data is independent of the skin roughness and the Reynolds number Hence equation [2] becomes:

$$f = f_2\left(\frac{k_s}{D_H};\ \frac{h}{l}\right) \tag{5}$$

The results are presented in Figs. 4 where the friction factor f is plotted as a function of the relative roughness k_s/D_H and the slope is given in legend. For steep slopes (i.e. $\alpha > 25$ degrees, Fig. 4a), the experimental results show little correlation between the flow resistance, the relative roughness and the channel slope. With channel slopes ranging from 50 to 55 degrees, Fig. 4a indicates values of the friction factor in the range 0.17 to 5 with a mean value of about 1.0. Fig. 4b presents the data obtained with flat chutes (i.e. $\alpha < 12$ degrees) and indicates a good agreement between data obtained on model (Noori 1984) and on prototype (Grinchuk et al. 1977). The results show also an increase of the friction factor with the relative roughness that appears to be independent of the channel slope. And equation (5) can be correlated by:

$$\frac{1}{\sqrt{f}} = 1.42 * \ln\left(\frac{D_H}{k_s}\right) - 1.25 \qquad \text{(for flat slopes)} \tag{6}$$

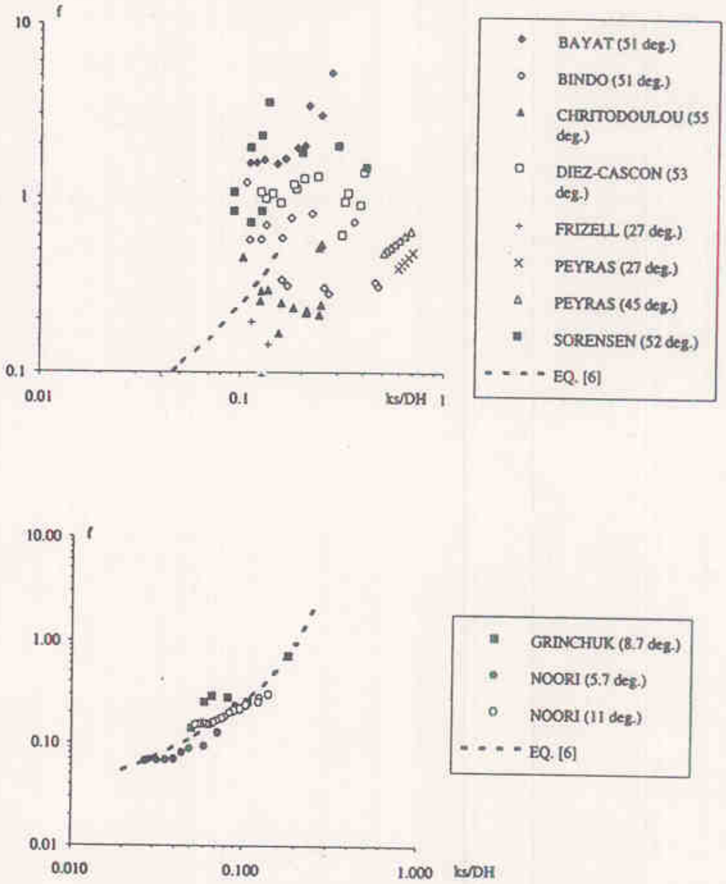

Fig. 4. Friction factors of stepped channels: (a) steep slopes (i.e. $\alpha > 27$ degrees); (b) flat slopes (i.e. $\alpha < 12$ degrees); Comparison with flows over rockfilled channels and triangular roughness (reference in Table 1).

It must be emphasised that the experimental data were analysed neglecting the effects of air entrainment. No information is available on the amount of air entrained during the experiments. The author believes that the flow depth measurements overestimated the clear water flow depth. As a result the values of the friction factor could be overestimated.

3.3 *Discussion*

A comparison between Figs. 4a and 4b shows a substantial increase of the friction factor when the channel slope increases from around 10 degrees (Fig. 4b) up to about 50 degrees (Fig. 4a). It is believed that such a difference is caused by different flow patterns in the recirculating cavity beneath the skimming stream.

For flat channels, the cavity of recirculating fluid between the edges of adjacent steps is oblong and large stable recirculation vortices cannot develop. The recirculating vortices do not fill the entire cavity between the edges, and the wake from one edge interferes with the next step as shown by photographs (Baker 1990) (Fig. 5b and 5c). The vortex generation and the dissipation process associated with each wake are disturbed by the next step and might interfere with those of the adjacent steps. The flow depth will control in part the vertical extent of the wake and the vortex interference region. The main flow parameters become the distance between two adjacent edges and the depth of flow. This reasoning is confirmed by the results shown on Fig. 4b which show a good correlation between the friction factor and k_s/D_H which is proportional to the edge spacing to flow depth ratio.

For very flat slopes, the flow pattern is characterised by the impact of the wake on the next step, a three-dimensional unstable recirculation in the wake and some friction drag on the step downstream of the wake impact (Fig. 5b). This flow pattern is called a "wake-step interference" regime. For larger slopes, the tail of the wake starts interfering with the next wake (Fig. 5c) and the friction drag component disappears. This pattern is called a "wake-wake interference" regime.
For steep slopes, a stable recirculation in the cavities between adjacent steps is observed as shown by photographs (Peyras et al. 1991, Diez-Cascon et al. 1991). The recirculating vortices are large two-dimensional vortices (Fig. 5a). The flow resistance is a function of the energy required to maintain the circulation of these large-scale vortices.
With strip roughness, Adachi (1964) and Knight and MacDonald (1979) observed a stable recirculation mechanism when the groove height to length ratio of the cavity was larger than 0.4. Other researchers (Maull and East 1963, Kistler and Tan 1967) studied flows in rectangular cavities with various aspect ratio. They observed stable recirculatory flow patterns for height-length ratio larger than 0.4 to 0.45. For a stepped spillway, the cavity height to length ratio equals:

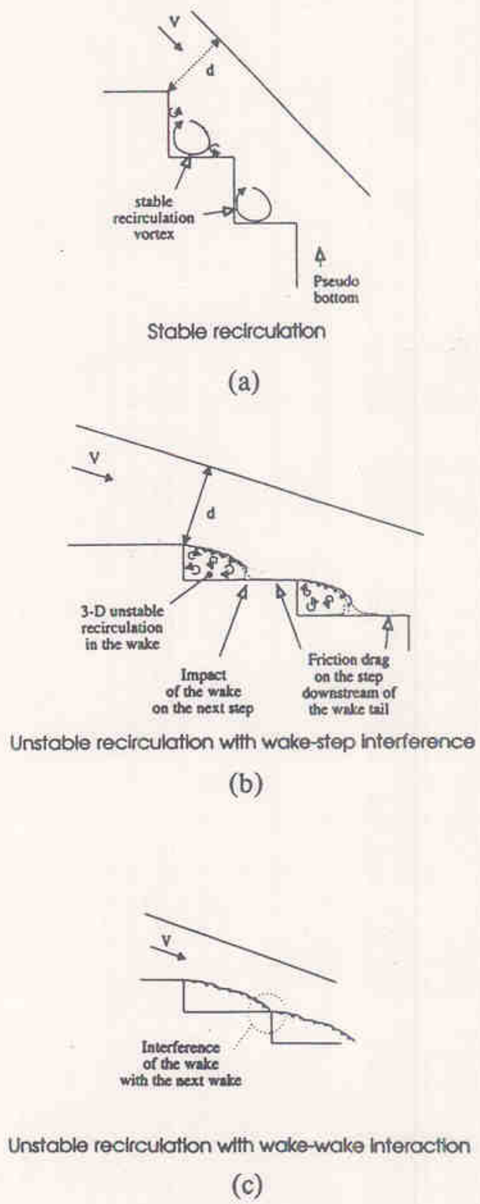

Fig. 5. Recirculation in the cavity between adjacent steps.

[$\cos\alpha * \sin\alpha$] and this value of 0.4 would correspond to a channel slope $\alpha = 26.6$ degrees. The results of Maull and East (1963), Adachi (1964), Kistler and Tan (1967) and Knight and MacDonald (1979) would imply that stable recirculation occurs for slopes larger than 26.6 degrees on a stepped chute. A comparison between Figs. 4a and 4b indicates clearly a different flow resistance behaviour for channel slopes larger than 27 degrees, and this is coherent with the findings of these researchers.

For slopes around 27 degrees, the flow pattern is most probably characterised by the interference of the wake tail with the next wake (Fig. 5c). Note that there is little data available for slopes between 15 to 45 degrees.

3.4 *Analogy with flows over large roughness*

Fig. 6 compares experimental data obtained on stepped chutes with flat slopes (i.e. $\alpha < 12$ degrees), on rockfilled channels and over large roughness (Table 3). All the sets of data indicate the same trend: i.e., the friction factor increases with the relative roughness.

Flows over rockfilled channels do not exhibit steady stable recirculating flow motion but unstable vortices behind rocks. These three-dimensional unstable flow patterns have some similarity with the flow patterns above flat stepped channels. This may explain the good correlation in values of friction factors (Fig. 6). Fig. 6 shows also a good agreement between the experiments on stepped channels and experiments over large roughness. It is thought that these flows have similar patterns and are dominated by unstable recirculating eddies and wake interference processes.

Considering steep stepped channels, the large-scale recirculating vortices play a major role in dissipating the flow energy. As a result, the friction factor results show an apparent lack of correlation with the Reynolds number and the relative roughness. A similar result was noticed by Perry et al. (1969) who analysed velocity profiles in developing boundary layers in arbitrary pressure gradients.

It is worth noting that Rajaratnam (1990) compared experiments in stepped channels with experimental results obtained with steeppass and Denil fishways. His analysis showed that the friction factors for fishways are of the same order of magnitude as for stepped channels. For steeppass fishways, Rajaratnam and Katopodis (1991) obtained friction factors in the range 0.4 to 4.

3.5 *Velocity distribution*

Frizell (1992) performed velocity measurements for a channel slope of 27 degrees and with horizontal steps. The measurements were obtained in the gradually varied flow region. A re-analysis of the data indicates that the velocity distributions follow a power law and that the exponent of the velocity distribution is about: $N = 3.5$.

For uniform non-aerated flows, Chen (1990) derived a theoretical relation between the exponent N and the friction factor as

$$N = K * \sqrt{\frac{8}{f}} \tag{7}$$

where K is the Von Karman constant ($K = 0.4$). For Frizell's (1992) experiments, equation (7) would imply: $f = 0.10$. Such a value is of the same order of magnitude as the experimental values deduced from equation (4) (i.e. f between 0.09 and 0.18, Fig. 4a).

Table 3. Experiments of flows over large roughness
Expérimentations d'écoulements avec de grandes rugosité

reference	slope (deg.)	discharge q_w (m^2/s)	relative roughness k_s/D_H	*Re*	remarks
Flows over strip roughness					
Bazin (1865)	0.086 to 0.51	0.046 to 0.62	0.0077 to 0.055	1.6E+5 to 1.9E+6	Wooden rectangular strips: $k_s=10$ mm, $l_s=27$ mm, $L_s=37$ mm. $W=1.98$ m. Channel length > 200 m.
Skoglund (1936)			0.008 to 0.06	4E+3 to 2.5E+5	Wide rectangular brasss pipes. 60-degree V-grooves: $k_s=0.32$ mm, $L_s=1.52$ mm.
Streeter and Chu (1949) (a) (b)			0.0112 & 0.0204	2E+5 to 8E+5	Circular aluminium pipe (ø = 0.114 m) with square threads.
Adachi (1964)	0.11	7.5E-4 to 0.075	0.023 to 0.48		Wooden rectangular bars: $k_s=5$ mm, $l_s=6.4$ mm, $W=0.20$ m.
Perry et al. (1969)					Recirculating wind tunnel. $k_s=3.2$, 12.7 and 25.4 mm. $l_s=25.1$, 12.7 and 22.3 mm. $L_s/k_s=1.83$ and 9.
Knight and MacDonald (1979)	0.055	0.008 to 0.19	0.006 to 0.021	2.7E+4 to 3.2E+5	Square perspex strip roughness: $k_s=3$ mm, $l_s=3$ mm, $W=0.46$ m.
Flow over roughness elements					
Sayre and Albertson (1963)	0.06 to 0.17	0.02 to 0.07	0.05 to 0.14	8.3E+4 to 2.5E+5	Baffle blocks: $k_s=38$ mm, $L_s=76$ mm, width = 152 mm. $W=2.44$ m.
O'Loughlin and MacDonald (1964)	0 to 2	up to 0.125	0.023 to 0.083		Cubical roughness elements: $k_s=12.7$ mm. Spacing: 1.4 to $9*k_s$. $W=0.61$ m.
Flows over triangular roughness					
Vittal et al. (1977)			0.05 to 0.13	3.2E+4 to 2.6E+5	Flat open channel with two-dimensional triangular roughness elements:  Roughness height: $k_s=0.03$ m. Height-length ratio: 1/5. $W=0.6$ m.
Gevorkyan and Kalantarova (1992)			0.05 to 0.125		Stepped teeth directed against the flow:  Height-length ratio: 1/4. Zemarin's formula.
Rockfilled channels					
Judd and Peterson (1969)	0.5 to 3.8	0.06 to 3	0.04 to 0.72	1.9E+5 to 8.8E+6	Field data. Natural torrents in USA.
Hartung and Scheuerlein (1970)	6 to 34		0.02 to 0.2	8.5E+4 to 2E+6	Model study. Artificial rockfilled channel, Germany.
Bathurst (1978)	0.5 to 1	0.06 to 0.37	0.11 to 0.34	2.1E+5 to 1.4E+6	Field data. Natural streams in England.
Thompson and Campbell (1979)	0.2 to 3	0.3 to 7.7	0.014 to 0.15	1.2E+6 to 2.8E+7	Field data. Torrents in USA and rockfilled channels in New Zealand.
Bathurst (1985)	0.23 to 2.2	0.02 to 4.9	0.012 to 0.25	9.5E+4 to 1.7E+7	Field data in United Kingdom.
Thorne and Zevenbergen (1985)	0.8 to 1.1	0.15 to 0.9	0.065 to 0.11	6E+5 to 3.5R+6	Field data. Mountain river in Colorado, USA.

Note: *Re*: Reynolds number: $Re=\varrho_w*U_w*D_H/\mu_w$.
(a): circular pipe flows; (b): as reported in Perry et al. (1969).

4 Point of inception of air entrainment

For a stepped spillway, the aerated flow region follows a region where the free surface of the flow is smooth and glassy (Fig. 1). However turbulence is generated next to the boundary and the turbulent boundary layer grows until the outer edge reaches the free surface. When the outer edge of the boundary layer reaches the free surface, the turbulence can initiate natural free surface aeration (Fig. 1). The location of the start of air entrainment is called the point of inception, and its characteristics are L_I and d_I. L_I is the distance from the start of the growth of the boundary layer and d_I is the depth of flow at the point of inception. For smooth spillways, Wood et al. (1983) showed that the flow properties at the point of inception can be estimated as:

$$\frac{L_I}{k_s} = 13.6 * (\sin\alpha)^{0.0796} * (F*)^{0.713} \tag{8}$$

$$\frac{d_I}{k_s} = \frac{0.223}{(\sin\alpha)^{0.04}} * (F*)^{0.643} \tag{9}$$

where $F*$ is defined as: $F* = q_w / \sqrt{g * \sin\alpha * k_s^3}$.

For stepped spillway, most designs of the ogee crest are fitted to a Creager profile (e.g. M'Bali dam) or a WES profile (e.g. Monksville dam). Usually few smaller steps are introduced near the crest to eliminate deflecting jets of water (Fig. 1). With such a geometry, the analysis of the growth of the boundary layer becomes extremely complex.

The author analysed the flow properties at the point of inception using model data. The results are presented on Fig. 7. in summary the flow properties can be estimated as:

$$\frac{L_I}{k_s} = 9.8 * (\sin\alpha)^{0.080} * (F*)^{0.71} \tag{10}$$

$$\frac{d_I}{k_s} = \frac{0.40}{(\sin\alpha)^{0.04}} * (F*)^{0.64} \tag{11}$$

where $k_s = h * \cos\alpha$. Equation (10) and (11) are shown on Fig. 6. A comparison between equations (8) and (10) indicates that the smooth spillway calculations (equation (8)) would overestimate the distance of the apparition of "white waters" on stepped chutes.

It must be emphasised that equations (10) and (11) were deduced from data obtained with channel slopes ranging from 27 to 52 degrees. Great care must be taken when using these equations with different slopes.

Discussion of the effects of air entrainment

Downstream of the point of inception, air is entrained at the free surface. A mixture of air and water extend gradually through the fluid. Far downstream, the flow will become uniform.

The author (Chanson 1993) showed that the drag reduction observed with air entrainment reduces the energy dissipation above the chute and hence the spillway efficiency. For slopes larger than 30 degrees, the effects of air entrainment can no longer be neglected for the computations of the residual flow energy at the downstream end of the spillway.

6 Conclusion

Over the recent decades, stepped chutes have become more popular. But there is a lack of knowledge on the hydraulics of skimming flows. This paper describes some characteristics of

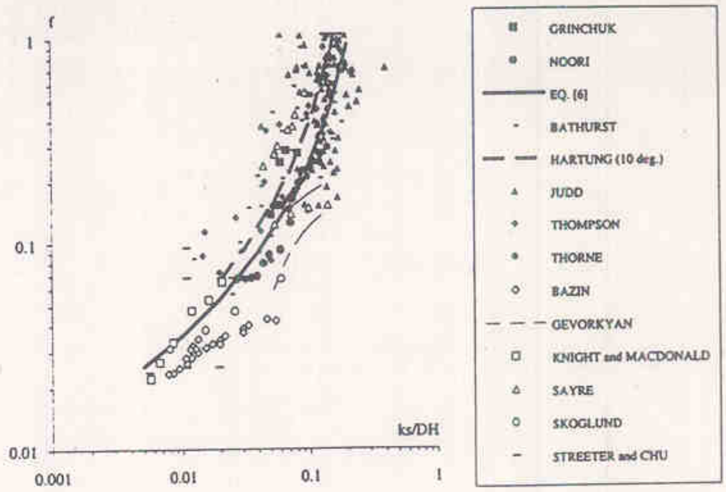

Fig. 6. Comparison between flow resistance of stepped spillways (flat slopes), large roughness and rock-filled channels (references in Table 3).

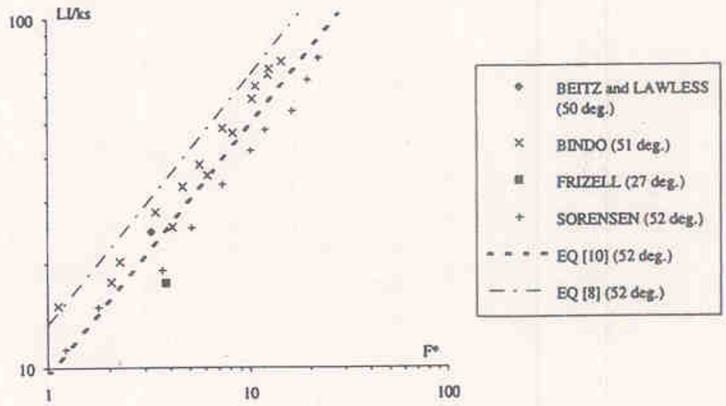

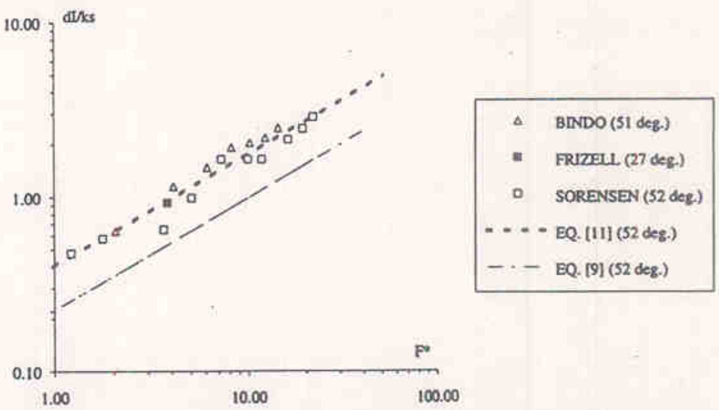

Fig. 7. Caracteristics of the point of inception: (a) distance from the spillway crest; (b) flow depth.

skimming flows on stepped chutes. Firstly the conditions of apparition of skimming flow are detailed (eq. [1]). Then new results are presented to estimate the flow resistance along stepped chutes. The study indicate some distinction between the flow resistance over steep and flat stepped chutes: i.e. slopes smaller or larger than 27 degrees. It is believed that the difference coincides to different flow patterns in the cavity of recirculating fluid between adjacent steps (Fig. 5). Some analogy with flows over large roughness is also developed. For flat slopes, an empirical correlation is presented (equation (6)). For steep slopes, the data show a wide scatter with mean friction factor of the order of magnitude of unity. Later the flow conditions at the start of air entrainment are described. The results indicate that free surface aeration occurs much upstream than on smooth spillways.

This study shows that further experimental work is required. In particular there is no information on the flow characteristics between the inception point of air entrainment and the uniform flow region.

More new prototype data are required for steep slopes.

Notations

D_H	hydraulic diameter (m)
d	flow depth (m) measured normal to the channel slope at the edge of a step
d_I	flow depth at the inception point (m)
d_c	critical flow depth (m)
$(d_c)_{onset}$	critical flow depth (m) at the onset of skimming flows
d_0	uniform flow depth (m) also called normal depth
$F*$	Froude number defined as: $F* = q_w/\sqrt{g*\sin\alpha*k_s^3}$
f	friction factor of non-aerated flow
g	gravity constant (m/s^2)
H	total head (m)
h	height of steps (m)
K	Von Karman universal constant
k_s	1-roughness height (m)
	2-step dimension normal to the flow: $k_s = h*\cos\alpha$
k'_s	equivalent uniform sand roughness of the channel surface (m)
L_I	distance from the start of growth of boundary layer to the point of inception (m)
L_s	roughness spacing (m)
l	horizontal length of steps (m)
l_s	roughness length (m)
N	exponent of the velocity power law
Q_w	water discharge (m^3/s)
q_w	water discharge per unit width (m^2/s)
Re	Reynolds number defined as: $Re = \rho_w * U_w * D_H/\mu_w$
s	curvilinear coordinate (m): i.e. distance (m) along the channel from the crest
U_w	flow velocity (m/s): $U_w = q_w/d$
W	channel width (m)
α	spillway slope
μ_w	dynamic viscosity of water (N.s/m^2)
ρ_w	density of water (kg/m^3)

References / Bibliographie

Adachi, S. (1964), On the Artificial Roughness, Disaster Prevention Research Institute Bulletin, No. 69, Kyoto University, Japan, March, 20 pages.

Baker, R. (1990), Precast Concrete Blocks for High Velocity Flow Applications, J. Iwem, Vol. 4, Dec., pp. 552–557, Discussion: Vol. 4, pp. 557–558.

Bathurst, J. C. (1978), Flow Resistance of Large-Scale Roughness, J. of Hyd. Div., ASCE, Vol. 104, No. HY12, pp. 1587–1603.

Bathurst, J. C. (1985), Flow Resistance Estimation in Mountain Rivers, J. of Hyd. Engrg., ASCE, Vol. 111, No. 4, pp. 625–643.

Bayat, H. O. (1991), Stepped Spillway Feasibility Investigation, Proc. of the 17th ICOLD Congress, Vienna, Austria, Q.66, R.98, pp. 1803–1817.

Bazin, H. (1865), Recherches Expérimentales sur l'Ecoulement de l'Eau dans les Canaux Découverts, (Experimental Research on Water Flow in Open Channels), Mémoires présentés par divers savants à l'Académie des Sciences, Paris, France, Vol. 19, pp. 1–494 (in French).

Beitz, E. and Lawless, M. (1992), Hydraulic Model Study for dam on GHFL 3791 Isaac River at Burton Gorge, Water Resources Commission Report, Ref. No. REP.24.1, Sept. Brisbane, Australia.

Bindo, M., Gautier, J. and Lacroix, F. (1993), The Stepped Spillway of M'Bali Dam, Intl Water Power & Dam Construction, Vol. 45, No. 1, pp. 35–36.

Chanson, H. (1993), Stepped Spillway Flows and Air Entrainment, Can. J. of Civil Eng., June.

Chen, C. L. (1990), Unified Theory on Power Laws for Flow Resistance, J. of Hyd. Engrg., ASCE, Vol. 117, No. 3, pp. 371–389.

Christodoulou, G. C. (1993), Energy Dissipation on Stepped Spillways, J. of Hyd. Engrg., ASCE, Vol. 119, No. 5, pp. 644–650.

Degoutte, G., Peyras, L. and Royet, P. (1992), Skimming Flow in Stepped Spillways – Discussion, J. of Hyd. Engrg., ASCE, Vol. 118, No. 1. pp. 111–114.

Diez-Cascon, J., Blanco, J. L., Revilla, J. and Garcia, R. (1991), Studies on the Hydraulic Behaviour of Stepped Spillways, Intl Water Power & Dam Construction, Sept., pp. 22--6.

The Engineer (1939), The Ladaybower Reservoir, The Engineer, Vol. 168, pp. 440–442.

Essery, I. T. S. and Horner, M. W. (1978), The Hydraulic Design of Stepped Spillways, CIRIA Report No. 33, 3nd edition, Jan., London, UK.

Forbes, R. J. (1955), Studies in Ancient Technology, Leiden, E. J. Brill, 9 Vol.

Frizell, K. H. (1992), Hydraulics of Stepped Spillways for RCC Dams and Dam Rehabilitations, Proc. of the 3rd Specialty Conf. on Roller Compacted Concrete, ASCE, San Diego CA, USA, pp. 423–439.

Frizell, K. H. and Mefford, B. W. (1991), Designing Spillways to Prevent Cavitation Damage, Concrete International, Vol. 13, No. 5, pp. 58–64.

Gasparotto, R. (1992), Waterfall Aeration Works, Civil Engineering, ASCE, Oct., pp. 52–54.

Gevorkyan, S. G. and Kalantarova, Z. K. (1992), Design of Tsunami-Protective Embankments with a Complex Front Surface, Gidrotekhnicheskoe Stroitel'stvo, No. 5, May, pp. 19–21 (Hydrotechnical Construction, 1992, Plenum Publ., pp. 286–290).

Grinchuk, A. S., Pravdivets, Y. P. and Shekhtman, N. V. (1977), Test of Earth Slope Revetments Permitting Flow of Water at Large Specific Discharges, Gidrotekhnicheskoe Stroitel'stvo, No. 4, pp. 22–26 (in Russian). (Translated in Hydrotechnical Construction, 1978, Plenum Publ., pp. 367–373).

Hartung, F. and Scheuerlein, H. (1970), Design of Overflow Rockfill Dams, Proc. of the 10th ICOLD Congress, Montréal, Canada, Q.36, R.35, pp. 587–598.

Henderson, F. M. (1966), Open Channel Flow, MacMillan Company, New York, USA.

Judd, H. E. and Peterson, D. F. (1969), Hydraulics of Large Bed Element Channels, UWRL Research Report, PRG 17-6, Utah State University, Logan, USA, 115 pages.

Kistler, A. L. and Tan, F. C. (1967), Some Properties of Turbulent Separated Flows, Physics of Fluids, Vol. 10, No. 9, Pt II, pp. S165–S173.

Knight, D. W. and MacDonald, J. A. (1979), Hydraulic Resistance of Artificial Strip Roughness, J. of Hyd. Div., ASCE, Vol. 105, No. HY6, June, pp. 675–690.

Krest'yaninov, A. N. and Pravdivetss, Y. P. (1986), Stepped Spillways for Small Dams, Gidrotekhnicheskoe Melioratsiya, No. 8, pp. 27–30 (in Russian).

Levin, L. (1968), Formulaire des Conduites Forcées, Oléoducts et Conduits d'Aération, (Handbook of Pipes, Pipelines and Ventilation Shafts), Dunod, Paris, France (in French).

Maull, F. J. and East, L. F. (1963), Three-Dimensional Flow in Cavities, J. of Fluid Mech., Vol. 16, pp. 620–632.

NOORI, B. M. A. (1984), Form Drag Resistance of Two Dimensional Stepped Steep Open Channel, Proc. of the 1st Intl Conf. on Hyd. Design in Water Resources Engineering, Channels and Channel Control Structures, Southampton, UK, K. V. H. Smith (ed.), Springer-Verlang Publ., pp. 1.133–1.147.

O'LOUGHLIN, E. M. and MACDONALD, E. G. (1964), Some Roughness Concentration Effects on Boundary Resistance, J. La Houille Blanche, No. 7, pp. 773–783.

PERRY, A. E., SCHOFIELD, W. H. and JOUBERT, P. N. (1969), Rough Wall Turbulent Boundary Layers, J. of Fluid Mech., Vol. 37, Part 2, pp. 383–413.

PEYRAS, L., ROYET, P. and DEGOUTTE, G. (1991), Ecoulement et Dissipation sur les Déversoirs en Gradins de Gabions, (Floows and Dissipation of Energy on Gabion Weirs), J. La Houille Blanche, No. 1, pp. 37–47 (in French).

PEYRAS, L., ROYET, P. and DEGOUTTE, G. (1992), Flow and Energy Dissipation over Stepped Gabion Weirs, J. of Hyd. Engrg., ASCE, Vol. 118, No. 5, pp. 707–717.

PRAVDIVET, Y. P. and BRAMLEY, M. E. (1989), Stepped Protection Blocks for Dam Spillways, Intl Water Power & Dam Construction, July, pp. 49–56.

RAJARATNAM, N. (1990), Skimming Flow in Stepped Spillways, J. of Hyd. Engrg., ASCE, ol. 116, No. 4, pp. 587–591.

RAJARATNAM, N. and KATOPODIS, C. (1991),, Hydraulics of Steeppass Fishways, Can. J. of Civil Eng., Vol. 18, pp. 1024–1032.

SAYRE, W. W. and ALBERTSON, M. L. (1963), Roughness Spacing in Rigid Open Channels, Transactions, ASCE, Vol. 128, pp. 343–372, Discussion: Vol. 128, pp. 372–427.

SKOGLUND, V. J. (1936), Effect of Roughness on the Friction Coefficient of a Closed Channel, J. of Aeronaut. Sciences, Vol. 4, Nov., pp. 28–29.

SMITH, N. (1971), A History of Dams, The Chaucer Press, Peter Davies, London, UK.

SORENSEN, R. M. (1985), Stepped Spillway Hydraulic Modxel Investigation, J. of Hyd. Engrg., ASCE, Vol. 111, No. 12, pp. 1461–1472.

STEIN, A. (1990), Surveys on the Roman Frontier in Iraq and Trans-Jordan, The Geographical Journal, Vol. XCV, pp. 428–438.

STREETER, V. L. and CHU, H. (1949),Fluid Flow and Heat Transfer in Aritificially Roughened Pipes, Report Project 4918, Armour Research Foundation, Chicago, USA.

THOMPSON, S. M. and CAMPBELL, P. L. (1979), Hydraulics of a Large Channel Paved with Boulders, J. of Hyd. Res., IAHR, Vol. 17, No. 4, pp. 341–354.

THORNE, C. R. and ZEVENBERGEN, L. W. (1985),Estimating VVelocity in Mountain Rivers, J. of Hyd. Engrg., ASCE, Vol. 111, No. 4, pp. 612–624.

VITTAL, N., RANGA RAJU, K. G. and GARDE, R. J. (1977), Resistance of Two Dimensional Triangular Roughnesss, J. of Hyd. Res., IAHR, Vol. 15, No. 1, pp. 19–36.

WEGMANN, E. (1907),The Dessign of the New Croton Dam, Transaction, ASCE, Vol. LXVIII, No. 1047, pp. 398–457.

WOOD, I. R., ACKERS, P. and LOVELESS, J. (1983), General Method for Critical Point on Spillways, J. of Hyd. Eng., ASCE, Vol. 109, No. 2, pp. 308–312.